

# Digital Tuning as an Exploratory Tool in the Modal Analysis of Randomly-Loaded Vibrating Structures

D. R. CRUISE\* AND R. G. CHRISTIANSEN†  
Naval Weapons Center, China Lake, Calif.

A heuristic approach to the analysis of multichannel experimental data such as that obtained from vibrating structures is presented. The spatial covariance matrix, the Fourier transformation, and notions from factor analysis are used to obtain approximate mode shapes and natural frequencies for structures responding to random loadings. This approach is demonstrated using experimental data obtained from the response of a long cantilevered cylindrical shell subjected to random loading.

## Nomenclature

$A, a_{ij}$	= complex Fourier amplitudes
$B, b_{jj}$	= $b_{jj}^2 = d_{jj}$
$C$	= strictly defined, spatial covariance matrix ( $C = 1/mV$ )
$\text{cis } z$	= $\cos z + (-1)^{1/2} \sin z$
$D, d_{jj}$	= diagonal matrix containing the eigenvalues of $F'F$
$E$	= Young's modulus
$F(t, x)$	= forcing function
$F, f_{ij}$	= data matrix obtained from the experiment
$f(t, x)$	= generalized amplitude function sampled to obtain $F$
$G, g_k(t_i)$	= modal signals
$H, h_k(x_j)$	= mode shapes (normalized)
$I$	= area moment of inertia
$L$	= length of beam
$m$	= number of times at which $f(t, x)$ is sampled
$N_k$	= noise estimated for mode $k$
$n$	= number of places at which $f(t, x)$ is sampled
$P$	= orthogonal matrix approximating $G$
$Q$	= orthogonal matrix approximating $H$
$SSA$	= sum of squared amplitudes
$S_k$	= signal strength estimated for mode $k$
$\text{Tr}(V)$	= trace of $V$ (sum of diagonal elements)
$t$	= time
$U_k$	= covariance matrix lacking certain frequency information
$V, v_{ik}$	= spatial covariance matrix ( $F'F, A^*A$ )
$V_k$	= covariance matrix for a specified frequency range
$W, w_{ij}$	= unitary Fourier transformation matrix
$W^*$	= inverse Fourier transform
$X_k$	= linear combinations
$x$	= generalized geometric site
$\Delta t$	= time between sampling
$\lambda$	= signal-to-noise ratio
$\mu$	= mass per unit length
$\omega_k$	= frequency of mode $k$

## Superscripts

'	= transposed matrix
*	= transposed, complex conjugate matrix

## Subscripts

$i, j, k$	= dummy indices
-----------	-----------------

## Introduction

THIS paper presents data reduction methods which extract modal information from the experimental responses of randomly loaded vibrating structures. The basic assumption is

that a function of two variables (such as structural response at time  $t$  and location  $x$ ) can be expressed in terms of functions of a single variable

$$f(t, x) = \sum_{k=1}^{\infty} h_k(x)g_k(t) \quad (1)$$

However, all analytic functions of two variables may be expressed by Eq. (1) within regions of convergence. To prove this, observe that the set of possible solutions includes the bivariate Taylor expansion.

A second assumption is that a finite lattice of points,  $t_i$  and  $x_j$ , can be chosen which adequately describes the function  $f(t, x)$

$$f(t_i, x_j) = \sum_{k=1}^n h_k(x_j)g_k(t_i) \quad \begin{cases} 1 \leq j \leq n \\ 1 \leq i \leq m \end{cases} \quad (2)$$

In Eq. (2) the number of terms need not exceed  $m$  or  $n$  which-ever is smaller.

When the functions,  $h_k(x)$  are orthogonal,  $h_k(x)$  and  $g_k(t)$  may be determined by a technique called factor analysis.<sup>1,2</sup> When the functions are not orthogonal (or when proper lattice points cannot be chosen) another technique termed digital tuning can be applied. It requires that the functions,  $g_k(t)$ , have a character which can be recognized and isolated in the frequency domain.

The structure studied in the experimental part of this effort is a beamlike cantilevered cylinder. The response of beams is developed in several strengths of materials and vibration texts (e.g., Chen<sup>3</sup>). The results of these developments yield

$$EI(\partial^4 f / \partial x^4) + \mu(\partial^2 f / \partial t^2) = F(t, x) \quad (3)$$

where shear and rotary inertia have been omitted. Here,  $f = f(t, x)$ ,  $x$  is a position on the beam,  $E$  is Young's modulus,  $I$  is the area moment of inertia,  $\mu$  is the mass per unit length, and  $F(t, x)$  is the forcing function.

For free vibrations, the solution is

$$f(t, x) = \sum_{k=1}^n b_k(t)h_k(x) \quad (4)$$

where

$$b_k(t) = \sin \omega_k t \quad (5)$$

and  $h_k(x)$  is the shape of the  $k$ th mode. The mode shapes, which form an orthogonal set, and the natural frequencies  $\omega_k$  can be determined from Eq. (1) and the boundary conditions.<sup>3</sup>

If  $F(t, x)$  in Eq. (3) is a broadband, stationary, ergodic, random process, it has been shown by Eringen<sup>4</sup> that the solution to Eq. (1) is

$$f(t, x) = \sum_{k=1}^n g_k(t)h_k(x) \quad (6)$$

where the mode shapes  $h_k(x)$  are the same as those in Eq. (4).

Received March 12, 1973; revision received June 29, 1973.

Index categories: Structural Dynamic Analysis; Computer Technology and Computer Simulation Techniques; Aircraft Vibration.

\* Mathematician, Propulsion Development Department.

† Research Engineer, Propulsion Development Department.  
Member AIAA.

However, the modal signals,  $g_k(t)$  contain more complicated messages than the sinusoids,  $b_k(t)$ , in Eq. (4). The term "message" is not inappropriate because modulations in phase and amplitude betray the loadings and dampings provided the impulse response function of the structure is known.

The theory portion of this paper is more general than the experimental portion and can apply to any situation where the data take the form of Eq. (6), and the following assumptions are valid: 1) the process (stochastic or not) does not alter the form of the mode shapes  $h_k(x)$  and 2) the variables  $g_k(t)$  have a recognizable character, i.e., they are distinguishable in the frequency domain. Generally,  $h_k$  may be a vector and  $x$  may be a generalized site in three dimensions.

### Orthogonal Factor Analysis

The formalism of factor analysis is introduced to show how it can put experimental data into the form of Eq. (6). The array of data is obtained by sampling the structure undergoing complex motion at specified times  $t_i$  and at specified sites  $x_j$ . Thus the data matrix is formed

$$f_{ij} \equiv f(t_i, x_j) \quad \begin{cases} 1 \leq i \leq m \\ 1 \leq j \leq n \end{cases} \quad (7)$$

All points  $f_{ij}$ ,  $1 \leq j \leq n$  must correspond to a single time,  $t_i$ .

It is known that a real matrix  $F$  takes the form<sup>5,6</sup>

$$F = PBQ' \quad (8)$$

where  $P$  is an  $m$  by  $m$  orthogonal matrix,  $Q$  is an  $n$  by  $n$  orthogonal matrix, and  $B$  is defined

$$b_{ij} = \begin{cases} 0 & i \neq j \\ b_i & i = j \end{cases} \quad \begin{cases} 1 \leq i \leq m \\ 1 \leq j \leq n \end{cases} \quad (9)$$

The matrix  $Q$  may be determined by evaluating

$$F'F = QB'P'PBQ' = Q(B'B)Q' \quad (10)$$

The matrix

$$V = F'F \quad (11)$$

is a modified spatial covariance matrix. It is distinguished from the true spatial covariance matrix  $C$  by a scalar multiplier, i.e.,  $V = mC$ . Here it is seen that the positive, semidefinite matrix,  $F'F$ , is resolved into

$$F'F = QDQ' \quad (12)$$

where

$$D = B'B \quad (13)$$

is a diagonal matrix containing the eigenvalues of  $F'F$ . The columns of  $Q$  contain an orthogonal set of corresponding eigenvectors. The eigenvalues and corresponding eigenvectors are assumed to be sorted so that

$$d_{11} \leq d_{22} \leq \dots \leq d_{nn} \quad (14)$$

After  $Q$  has been determined, the matrix  $P$  may be found by

$$PB = FQ \quad (15)$$

which is taken from Eq. (8). The matrix  $B$  is easily removed from  $P$  but is left attached in the development which follows.

In the beam theory,<sup>3</sup> the mode shapes are orthogonal. Arbitrarily, they may also be normalized. These conditions are

$$\int_0^L h_k(x)h_l(x) dx = \begin{cases} 0 & k \neq l \\ 1 & k = l \end{cases} \quad (16)$$

where  $L$  is the length of the beam.

Next let it be assumed that discrete points

$$x_j \quad 1 \leq j \leq n \quad (17)$$

can be chosen, not knowing  $h_k(x)$  in advance, so that

$$\sum_{j=1}^n h_k(x_j)h_l(x_j) = \begin{cases} 0 & k \neq l \\ 1 & k = l \end{cases} \quad (18)$$

This is a critical assumption, often making factor analysis more ideal than practical. Note that the validity of Eq. (16) does not in itself assure the validity of Eq. (18).

The user assumes by the application of factor analysis that

$$F = (PB)Q' \quad (19)$$

can be directly related to

$$F = GH \quad (20)$$

which is Eq. (6) expressed as a matrix product.

That is, the matrix  $Q$  contains the normal modes  $h_k(x)$  predicted by Eq. (1), and  $PB$  contains the modal signals  $g_k(t)$ . Proof depends on the uniqueness of the form  $F = PBQ'$ . It has been shown by Eckart and Young<sup>5</sup> that this form is unique when no two nonzero elements of  $B$  are equal.

### Digital Tuning

Consider next the cases where it is not possible to obtain an orthogonal representation of the mode shapes [Eq. (18)]. Generally one has a structure of irregular geometry and of three-dimensional responses. An orthogonal representation may be impossible because of nonlinearity, out-of-plane coupling, data error, and the fact that the experimenter simply does not know the mode shapes in advance.

A nonorthogonal approach which uses Eq. (20) may be employed. The new analysis proceeds with the same motivation as in factor analysis; i.e., to find linear combinations of the multichannel output which are physically meaningful. If these linear combinations form a matrix  $X$  then

$$G(t) = FX \quad (21)$$

leads to the modal signals and the matrix  $X$  is identified from Eq. (20)

$$X = H^{-1} \quad (22)$$

The approach may first be described at the intuitive level by describing a possible analog computer experiment. Suppose the multichannel signals are inputted to the computer, each weighted by a variable factor, and the signals summed and displayed in the frequency domain. The operator has the advantage of knowing what a modal signal should look like. He adjusts the weights until one of the modal signals is isolated. The dial settings then provide a column of the  $X$  matrix.

In lieu of such analog equipment, the practicality of such an experiment has not been determined. However, a digital analysis isolates modal signals with insights revealed by the finite Fourier transformation.

The data matrix may be expressed

$$F = WA \quad (23)$$

where

$$w_{ij} = \frac{1}{(m)^{1/2}} \cos [2\pi(i-1)(j-1)/m] \quad \begin{cases} 1 \leq i \leq n \\ 1 \leq j \leq m \end{cases} \quad (24)$$

The columns of  $A$  differ from the Fourier transforms of the columns of  $F$  only by the factor  $(m)^{1/2}$ . This factor is introduced so that  $W$  is a "unitary" matrix

$$W^* = W^{-1} \quad (25)$$

Here the asterisk denotes the transpose of the complex conjugate. The covariance matrix may also be examined

$$V = F'F = A^*W^*WA = A^*A \quad (26)$$

This demonstrates that the same covariance matrix is obtained from the data and from its unitary transform. Hence

$$v_{ik} = \sum_{j=1}^m a_{ij}^* a_{jk} \quad \begin{cases} 1 \leq i \leq n \\ 1 \leq k \leq n \end{cases} \quad (27)$$

where the index  $j$  is related to frequencies as follows

$$\omega_j = 2\pi j / (n\Delta t) \quad (28)$$

and where  $\Delta t$  is the time between sampling.

Some further notations must be pursued before describing digital tuning. Consider the sum of squared amplitudes (SSA) of the acquired data

$$SSA = \sum_{i=1}^m \sum_{j=1}^n f_{ij}^2 \quad (29)$$

This is an important quantity which is related to the matrices:  $F'F = A^*A$ ,  $FF'$ , and  $AA^*$ . It is easily seen that the SSA is equal to the trace of  $V$

$$SSA = \sum_{i=1}^m \sum_{j=1}^n f_{ij}^2 = \sum_{k=1}^n v_{kk} = Tr(V) \quad (30)$$

It is interesting that the diagonal elements of  $V$  describe how the SSA is distributed among the geometric sites. For this reason  $V$  is termed the "spatial" covariance matrix.

It can be shown from orthogonal similarity<sup>7</sup> that

$$Tr(V) = Tr(F'F) = Tr(AA^*) \quad (31)$$

Inspection shows that the diagonal elements of  $FF'$  describe how the SSA is distributed among sample times,  $t_1, t_2, \dots, t_m$ . Further inspection shows that the diagonal elements of  $AA^*$  describe how the SSA is distributed among the frequencies of Eq. (28).

Reconsider the eigenrelation of  $V$  [Eq. (12)]. The trace theorem assures that the sum of the eigenvalues is also equal to the SSA

$$\sum_{k=1}^m d_{kk} = Tr(V) = SSA \quad (32)$$

In factor analysis, the eigenvalues describe how the SSA is distributed among the corresponding mode shapes.

More generally if  $H_k$  is a normalized mode shape, then

$$S_k = H_k' V H_k \quad (33)$$

is the portion of the SSA which can be attributed to it. But only for a complete, orthonormal set of eigenvector mode shapes,  $H_1, H_2, \dots, H_n$  do the  $S_k$  sum to the SSA.

It is possible to modify the spatial covariance matrix so that it contains information for a single specified range of frequencies. Hence

$$V(\omega_0 \leq \omega \leq \omega_1)$$

is obtained by modifying Eq. (27) so that the index  $j$  takes only the values

$$\omega_0 \leq \omega_j \leq \omega_1 \quad (34)$$

[where  $\omega_0$  and  $\omega_1$  may take only the discrete values allowed by Eq. (28)].

A second, modified matrix contains information for all frequencies except those in a certain range

$$U(\omega_0 < \omega < \omega_1) = V - V(\omega_0 < \omega < \omega_1) \quad (35)$$

Digital tuning may be described as follows. First inspect the diagonal elements of  $AA^*$  (Fig. 1). Peaks should indicate the modal signals as in the conventional analysis. Next determine frequency ranges for each mode  $k$

$$\omega_0(k) \rightarrow \omega_1(k) \quad (36)$$

which bracket the peaks. The more complicated the message, the broader these will be. Finally compute values of

$$V_k = V(\omega_0(k) \leq \omega \leq \omega_1(k)) \quad (37)$$

and

$$U_k = U(\omega_0(k) \leq \omega \leq \omega_1(k)) \quad (38)$$

The best estimate for the  $k$ th mode shape is obtained by finding the  $H_k$  for which

$$S_k = H_k' V_k H_k \quad (39)$$

is a maximum. This is because the quantity,  $S_k$ , is the portion of the SSA which is attributed to  $H_k$  in the frequency band considered. The problem is solved by equating  $H_k$  to the eigenvector of  $V_k$  which corresponds to the largest eigenvalue. This is actually a special factor analysis in which only one dominant factor is expected due to the mathematical foreplay shown in Eq. (37).

The linear combinations  $X_k$  [see Eq. (21)] which yield the modal signals are determined next. These should not only maximize the SSA associated with the  $k$ th frequency band

$$S_k = X_k' V_k X_k \quad (40)$$

but they should also minimize the noise coming from outside the frequency band

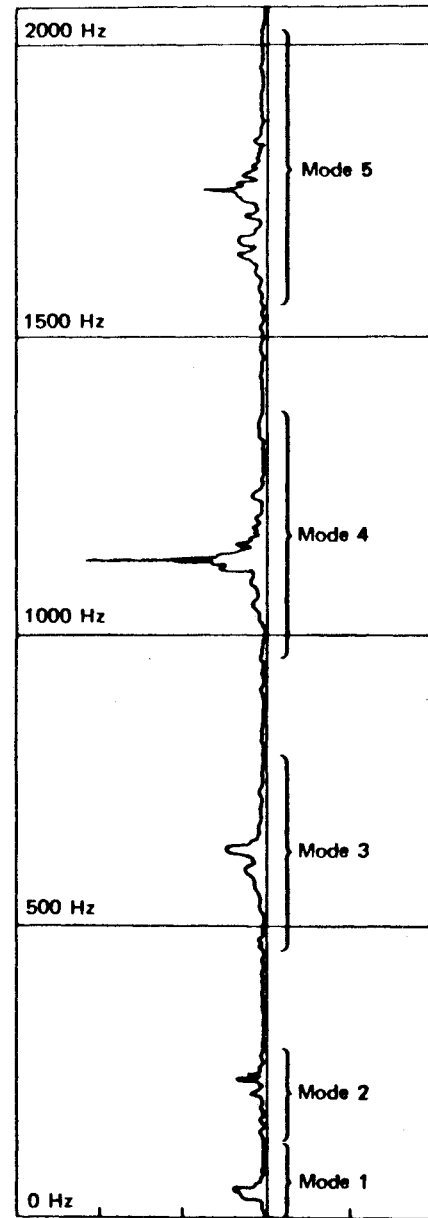


Fig. 1 Diagonal elements of  $AA^*$  from the experimental data.

Fig. 1 Diagonal elements of  $AA^*$  from the experimental data.

$$N_k = X_k' U_k X_k \quad (41)$$

The  $X_k$  should therefore be chosen so that the signal-to-noise ratio,  $\lambda_k = S_k/N_k$ , is a maximum. Equations (40) and (41) may be combined as follows

$$X_k' (V_k) X_k = X_k' (\lambda_k U_k) X_k \quad (42)$$

This may be solved by determining  $\lambda_k$  so that the largest eigenvalue of  $V_k - \lambda_k U_k$  is zero. The corresponding eigenvector is  $X_k$ .

It should be noted that the modal shapes and signals obtained from digital tuning only approximate Eq. (20) and that  $X$  is only an approximation to  $H^{-1}$  unless these matrices are orthogonal. If they are orthogonal, then factor analysis may be applied with less effort.

### Experimental Setup and Data Handling

The specimen used in this experiment was a beamlike right circular cylindrical shell with physical properties shown in Table 1. It was mounted in a cantilever (fixed-free) configuration and

Table 1 Physical properties of test beam

Material	2024 T-4 aluminum
Length, in.	70
Outside diameter, in.	5.000
Inside diameter, in.	4.910
Wall thickness, in.	0.094
Young's modulus ( $E$ ), lb/in.	$10.6 \times 10^6$

excited by randomly vibrating and fixed boundary to induce rigid body motion into the structure.

The autospectrum of the boundary motion was shaped and controlled using a Ling ASD/80 equalizer/analyzer (Fig. 2). This equalizer/analyzer is common to many environmental test laboratories and is capable of 25-Hz bandwidth control from 100 to 2000 Hz with finer bandwidth control below 100 Hz. The electrodynamic exciter and power amplifier were Ling Models A300 and 10/16, respectively. The input boundary motion control accelerometer (Fig. 3) was an Endevco Model 2270 used in conjunction with an Endevco Model 2713 charge amplifier. During the experiment, the calibration sensitivity for each amplifier was selected such that the maximum sensitivity would be three times the anticipated over-all rms test level. This is important for signal clipping considerations and maximum signal-to-noise ratio. Endevco Model 2226 response accelerometers were used in all cases. The charge amplifiers used were also Endevco Model 2713. The over-all level of the input and the response accelerometers was monitored using a Ballantine true rms voltmeter, while a Tektronics oscilloscope was used to monitor the inputs and responses for waveform and possible clipping.

The inputs and responses were recorded on magnetic tape using an Ampex ES100 tape recorder. The record speed was 60 in./sec (FM record 108 kHz center frequency),  $\pm 40\%$  deviation which allowed maximum signal-to-noise ratio while providing digitizing flexibility for playback at slower tape speeds.

The analog-to-digital conversion process used in preparing the data for analysis in this experiment was to digitize all channels of data simultaneously using a series of sample and hold amplifiers. This provided time integrity between samples of the outputs from the several points on the structure. Additionally, care was taken to insure that the data were prepared such that trends and d.c. level shifts were not introduced while preparing the data.

### Results

The output signals from the eight accelerometers (Fig. 3) were digitized at 5000 samples per second. A time slice of 1024 points was chosen leading to the data matrix

$$f_{ij} \begin{cases} 1 \leq i \leq 1024 \\ 1 \leq j \leq 8 \end{cases}$$

which had the power spectral density shown in Fig. 1. Factor analysis was applied to this matrix and the results reported.<sup>8</sup> Although the factor analysis results were informative, it was felt

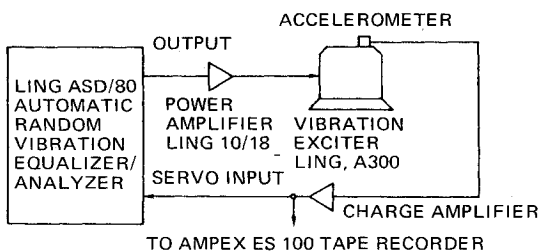


Fig. 2 Vibration control system.

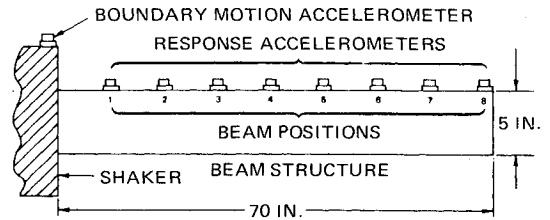
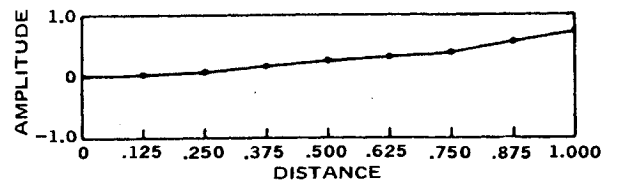


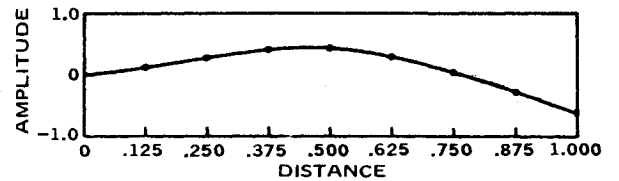
Fig. 3 Accelerometer location diagram.

that the finite representation did not quite lead to orthogonal mode shapes for the reasons discussed above and digital tuning was tried.

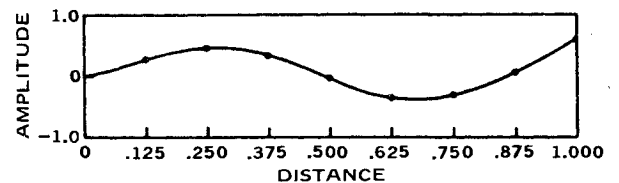
The 10 matrices, ( $V_k$ ;  $k = 1, 5$  and  $U_k$ ;  $k = 1, 5$ ), were computed from the data using Eqs. (35-38) for the frequency ranges shown



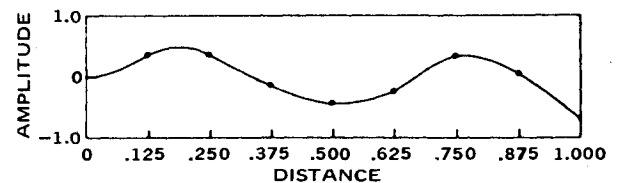
MODE NO. 1



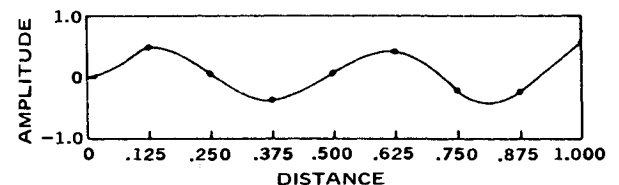
MODE NO. 2



MODE NO. 3



MODE NO. 4



MODE NO. 5

Fig. 4 Bending-mode shapes predicted from digital tuning.

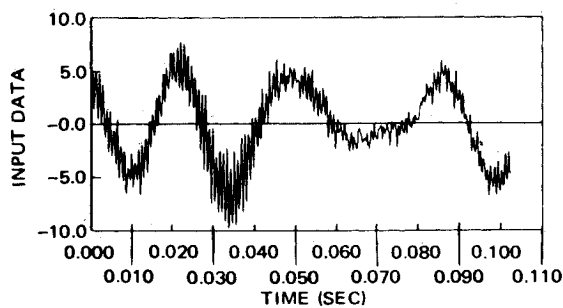


Fig. 5 Part of signal output from mode 1.

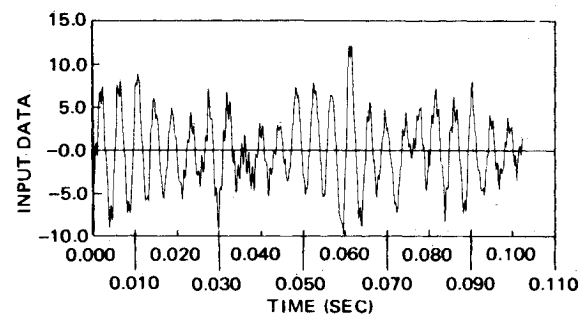


Fig. 6 Part of signal output from mode 2.

in Table 2. The five mode shapes obtained from Eq. (39) are shown in Table 3 and in Fig. 4. Note how the character of these curves agrees with theory.

Next, the linear combinations were computed from Eq. (42) and the modal signals computed from Eq. (21). Those for modes 1, 2, and 3 are shown in Figs. 5-7. The autocorrelations for modes 1, 2, and 3 are shown in Figs. 8-10. The autocorrelation curves were used to estimate the natural frequencies shown in Table 2. These are compared with the results of theory<sup>10</sup> in Table 4. Also shown in Table 2 are the signal-to-noise ratios computed from Eq. (42).

Table 2 Digital tuning summary

Mode no.	SSA (eigenvalues)	Frequency, Hz	Signal-to-noise ratio	Frequency range considered, Hz
1	22635	39.5	11.79	4.9- 117.3
2	14728	235.2	8.52	122.2- 410.6
3	45797	616.0	22.41	415.4- 826.0
4	385044	1,121.0	41.28	830.9-1,437.0
5	85537	1,669.0	102.6	1,441.8-2,497.6

Table 3 Mode shapes  $H_k$  computed from Eq. (39)

Beam position	Mode (normalized displacement)				
	No. 1	No. 2	No. 3	No. 4	No. 5
1	0.0036	0.1292	0.2849	0.3588	0.4926
2	0.0721	0.2696	0.4512	0.3378	0.0329
3	0.1471	0.4201	0.3566	-0.1498	-0.3961
4	0.2406	0.4439	-0.0398	-0.4194	0.0713
5	0.3065	0.3070	-0.3446	-0.0271	0.4201
6	0.3883	0.0711	0.3406	0.3456	-0.2327
7	0.5383	-0.2802	0.0630	0.0587	-0.2435
8	0.6168	-0.5995	0.5899	-0.6597	0.5517

Table 4 Comparison of theoretical and experimental modal frequencies

Mode no.	Bernoulli-Euler theory, Hz	Experiment results, Hz
1	40.5	39.5
2	257.0	235.0
3	707.0	616.0
4	1,375.0	1,121.0
5	2,190.0	1,669.0

## Discussion

The digital tuning method gives satisfactory results for 1) the case reported here, 2) other time slices from the same experiment, and 3) a small number of similar experiments. Although the method is promising, insufficient experiments have been run to establish the limits of its usefulness. It would appear, however, that the method is useful whenever the modal signals do not badly overlap in the frequency domain. A modal signal is not badly overlapped by other signals as long as one can find a frequency band [Eq. (37)] such that the signal-to-noise ratio in Eq. (42) is greater than two to one.

Digital tuning was applied recently to the three-dimensional outputs of a damped, three-gimbal structure. The results supported the hypothesis that digital tuning may be applied to very complicated situations and provide more information than conventional analyses.

There is an advantage and a disadvantage in the heuristic step of the method. The advantage is that the experimenter may interact with the data reduction procedure and thus gain insights. The disadvantage is that he may make errors in judgement as far as recognizing a modal signal. However, his judgement may be verified to some extent by the size of the signal-to-noise ratios obtained. It is also conceivable that the optimization of signal-to-noise ratio may be useful in separating partially overlapping signals.

The use of 1024 points in the time slice was arbitrary. No study of optimal time slice size has been made at this stage of development. However, when the loading is random, it is suspected that the larger the slice, the better the results within economic and core-size limitations. Actually the analysis discussed in this paper required 17 sec on the Univac 1108EDPM and sufficient core remained that a 4096 time slice could have been considered.

A computer program<sup>10</sup> has been developed that performs the calculations of this paper. It is conversational and may be used on a teletype or other interactive demand terminal for the Univac 1108EDPM.

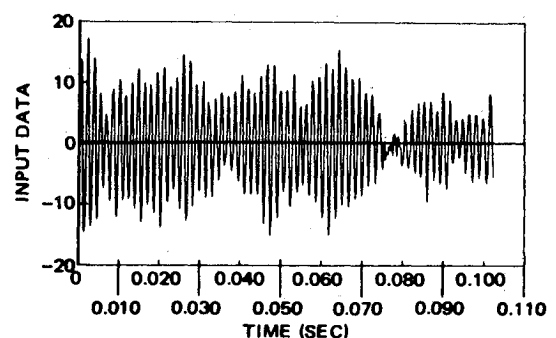


Fig. 7 Part of signal output from mode 3.

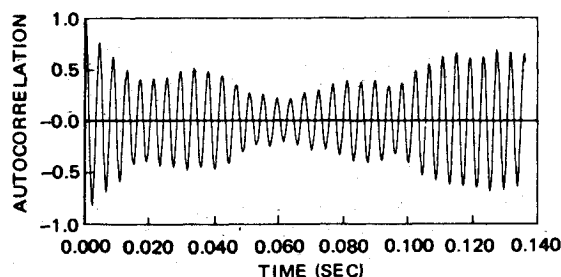


Fig. 9 Autocorrelation of mode 2.

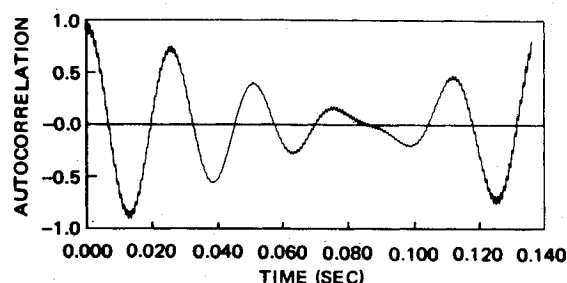


Fig. 8 Autocorrelation of mode 1.

### Appendix : Comparison of Digital Tuning and Digital Filtering

There are important similarities and differences between digital tuning and digital filtering. The most apparent difference is that digital tuning leads to mode shapes and digital filtering does not. This difference is not as essential as it may seem.

Consider a single channel of data which contains a number of definite messages carried in narrow frequency bands. A matrix  $F$  may be constructed which contains  $n$  pseudo channels

$$\begin{bmatrix} f_1 & f_2 & \cdots & f_n \\ f_2 & f_3 & \cdots & f_{n+1} \\ \vdots & \vdots & \ddots & \vdots \\ f_m & f_1 & \cdots & f_{n-1} \end{bmatrix} \quad (43)$$

The mathematics of digital tuning may be performed as before. In this case, no geometric significance may be placed on the mode shapes  $H_k$ . However,  $X_k$  may be used to perform a sliding analysis of the input data

$$g_k(t_i) = \sum_{j=1}^n x_{kj} f(t_{i+j}) \quad 1 \leq k \leq m \quad (44)$$

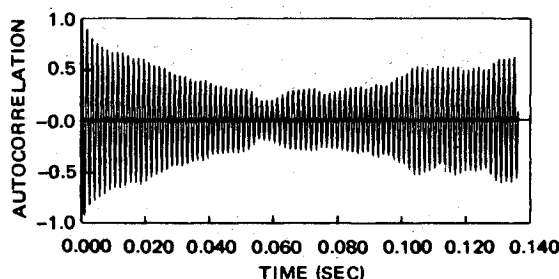


Fig. 10 Autocorrelation of mode 3.

and to obtain meaningful signals. This is similar to the weighting procedure of digital filtering.

When a data channel contains definite messages in narrow frequency bands, digital tuning is more efficient in that it tunes out only the competition that actually exists. Conceivably, the number of weighting coefficients may be as few as  $n$  which is the number of message signals. Digital filtering, on the other hand, must anticipate all frequencies outside the passed region.

As the data channel described in the foregoing approaches a white noise situation, digital tuning becomes asymptotic to digital filtering in its attempted task if not in its procedural approach.

### References

- Sheth, J. N., "Using Factor Analysis to Estimate Parameters," *Journal of American Statistics Association*, Vol. 64, Sept. 1969, pp. 808F and 822.
- Merkle, R. G., "Factor Analysis of Vibration Spectral Data from Multilocation Measurement," *Shock and Vibration Bulletin*, No. 42, Jan. 1972.
- Chen, Y., *Vibration: Theoretical Methods*, Addison-Wesley, Reading, Mass., 1966.
- Eringen, A. C., "Response of Beams and Plates to Random Loads," *Transactions of the ASME, Ser. E*, Vol. 24, No. 46, 1957, p. 46.
- Eckart, C. and Young, G., "The Approximation of One Matrix by Another of Lower Rank," *Psychometrika*, Vol. 1, No. 3, Sept. 1936, pp. 211-216.
- Householder, A. S. and Young, G., "Matrix Approximation and Latent Roots," *American Math Monthly*, Vol. 45, 1938, p. 165F.
- Perlis, S., *Theory of Matrices*, Addison-Wesley, Reading, Mass., 1952, p. 169ff.
- Christiansen, R. G. and Cruise, D. R., *Factor Analysis as an Exploratory Tool in the Modal Analysis of Randomly Loaded Vibrating Structures*, TP5373, Dec. 1972, Naval Weapons Center, China Lake, Calif.
- Timoshenko, S., *Vibration Problems in Engineering*, Wiley, New York, 1967.
- Christiansen, R. G. and Cruise, D. R., *Program for the Transformation and Manipulation of Digitized Periodic Data in Multichannel Arrays*, TP5451, April 1973, Naval Weapons Center, China Lake, Calif.